VTT Technical Research Centre of Finland

Millimeter-Wave Amplifier-Based Noise Sources in SiGe BiCMOS Technology

Forsten, Henrik; Saijets, Jan H.; Kantanen, Mikko; Varonen, Mikko; Kaynak, Mehmet; Piironen, Petri

Published in:
IEEE Transactions on Microwave Theory and Techniques

DOI:
10.1109/TMTT.2021.3104028

Published: 01/11/2021

Document Version
Peer reviewed version

Millimeter-Wave Amplifier-Based Noise Sources in SiGe BiCMOS Technology

Henrik Forstén, Jan Saijets, Mikko Kantanen, Mikko Varonen, Mehmet Kaynak, Petri Piironen

***Abstract*—This paper describes the development and characterization of wideband millimeter-wave noise sources based on SiGe BiCMOS amplifiers. Two single-ended three-stage amplifier-based noise sources reached excess noise ratio values over 20 dB from 120 to 220 GHz with 20 mA of bias current from a 2.3-volt supply. We also introduce a novel switchable noise source employing Lange coupler for providing wideband matching in both on and off configurations of the noise source. The Lange coupler-based noise source has better than 12-dB matching from 90 to 270 GHz with excess noise ratio of better than 15 dB from 125 to 235 GHz.**

***Index Terms*—millimeter-wave, noise sources, SiGe**

I. Introduction

Noise sources are important components for measuring noise figure of amplifiers and for calibrating radiometers. High excess noise ratio (ENR) noise sources have been used in noise figure measurements at least up to 200 GHz [1]. Noise sources have also been used as internal calibration target in radiometers of Jason [2] and SMOS [3] missions, for example.

Many noise sources are built using a diode in the avalanche breakdown region as it can generate a significant amount of wideband noise [4]–[6]. An amplifier with input termination can also be used as a noise source [7]. In this work we study the feasibility of implementing wideband noise sources using input terminated SiGe BiCMOS amplifiers. In addition to a good ENR performance, many applications require good matching in both on and off states of the noise source. Mismatch between on and off state impedances causes measurement uncertainty in noise figure measurements [9]. We introduce a novel noise source utilizing Lange coupler for wideband matching in both on and off configurations.

This paper is organized as follows. The design of a wideband input terminated amplifier-based noise source is presented in Section II A followed by the design of the novel Lange coupler-based noise source in Section II B. Measurement of all of the designed circuits are presented in Section III. Main findings are concluded in Section IV.

The manuscript of this paper was submitted for review on 2021-02-24; Revised 2021-06-04.

This work was supported by the European Space Research and Technology Centre (ESTEC), Noordwijk, the Netherlands under contract no. 4000122870/17/NL/HK. The work was also partially supported by the Academy of Finland Research Fellow project under Grant 310234

II. Circuit Design

The block diagram of the amplifier-based noise source is shown in Fig. 1. The noise source is a three-stage amplifier in cascode configuration with input terminated to an on-chip load.

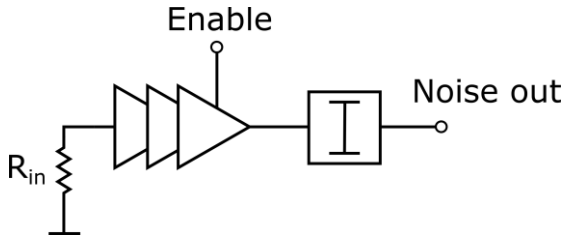

Fig. 1. Block diagram of the amplifier-based noise source which is an input terminated three-stage-amplifier having an attenuator at the output.

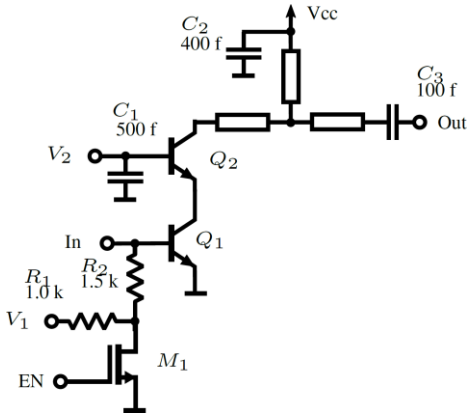

Fig. 2. Simplified schematic of the output stage.

The simplified schematic of the output stage is shown in Fig. 2. The bias of the cascode stage can be switched off using MOSFET M1, thus, enabling the cold load operation of the noise source. Switching off the first two stages is not necessary since the isolation of the last cascode stage is high enough to dampen the noise of the previous stages, so, that the cold noise temperature is in practice close to the ambient temperature. The hot noise temperature is controlled by adjusting the bias current

H. Forstén, J. Saijets, M. Kantanen and M. Varonen are with the MilliLab, VTT Technical Research Center of Finland, 02044 Espoo, Finland. (Corresponding author: Henrik Forstén.)

M. Kaynak is with IHP – Leibniz-Institut für innovative Mikroelektronik, 15236 Frankfurt (Oder), Germany.

Petri Piironen is with the European Space Agency (ESTEC), NL-2200 AG, Noordwijk, the Netherlands.

of all stages through current mirrors. The two first stages of the noise source are identical and similar on the schematic level to the output stage except for some differences in the transmission line lengths and there is no MOSFET for switching the bias. All of the transistors in all circuits have emitter area of $4\times(0.07\times0.9)\ \mu m^2$.

In addition to good ENR performance, our aim was to achieve good matching for the noise source design. Good matching is needed for noise sources that are for example intended for measuring the noise temperature of a stand-alone low-noise amplifier (LNA). In silicon technologies, the large RF pad capacitance makes it difficult to obtain wideband matching. This is because typically the RF probe pad is designed to have a ground plane under the pad which prevents the fields from entering the lossy and high dielectric constant silicon substrate. The ground plane under the pad forms a parasitic capacitor which at mm-wave frequencies affects the matching significantly. The parasitic capacitance can be compensated in narrow band using for example a shorted stub to resonate the capacitance out at single frequency. Compensation approaches don't offer very wide matching bandwidth and reducing the overall parasitics is necessary instead of trying to just compensate them. By removing the ground plane under the pad parasitic capacitance is significantly decreased increasing the bandwidth the pad can be used. The drawback is that the fields can enter the silicon which slightly increases the losses. The effect of the ground cutout was investigated using 3D electromagnetic (EM) simulations. The EM simulation model of the pad with the ground cut out is presented in Fig. 3. The input probe is modeled using a metal bridge and a lumped port. On the chip side wave port is used. Probe pitch is 100 µm and the center pad diameter is 80 µm. The simulation results are presented in Fig. 4. With the ground cutout, the matching is significantly improved compared to the same structure with a solid ground plane under the signal pad. At frequencies exceeding around 200 GHz the substrate losses start to increase quickly and smaller signal pad diameter and ground cutout would be needed. Another option is to use a floating shield structure as shown in Fig. 5. The floating shield isolates the silicon substrate with minimal parasitic capacitance. The smaller signal pad slightly improves the matching of the pad even further. The above assumptions are confirmed with simulations plotted in Fig. 4. The pad with floating shield and smaller pad has the widest bandwidth.

In the noise source design, the remaining pad capacitance is resonated out with a short-circuited shunt stub. To further improve the output matching an on-chip attenuator was added to the output of the noise source. Depending on design version it was either a conventional π-resistor connection or a shunt resistor to ground. It should be noted that although attenuator improves the matching and the noise source bandwidth it comes with the expense of reduced noise power.

The designs were implemented in IHP's SG13G2 130-nm SiGe process with f_t and f_{max} of 300 and 500 GHz, respectively.

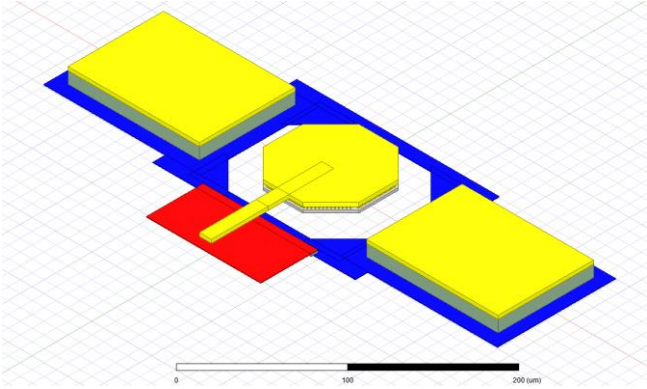

Fig. 3. EM simulation model of the GSG pad with ground cut out. Dielectric layers are not visible. The size of the center pad is 80 µm × 80 µm.

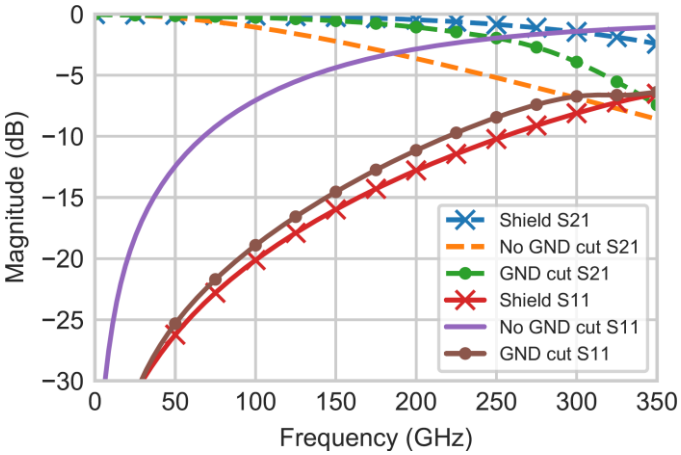

Fig. 4. GSG pad simulated S-parameters with and without ground cut out and with a smaller signal pad utilizing a floating shield.

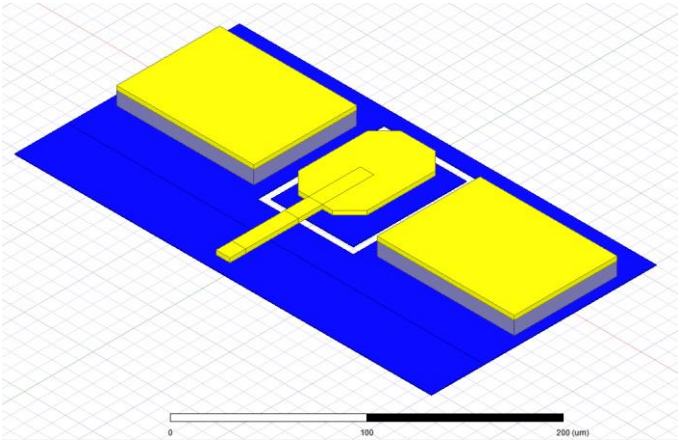

Fig. 5. EM simulation structure of the GSG pad with a small signal pad and floating shield underneath. The size of the center pad is 75 µm × 50 µm.

A. *Amplifier-based noise source*

Two versions of amplifier noise sources were designed with different size output pads and differently optimized inter-stage matching and line lengths. The first noise source version has the smaller output pad with floating ground shield below as in Fig. 5 whereas the second version utilizes the structure of Fig. 3 with ground cutout. The smaller output pad was also used to achieve smaller output capacitance and a larger bandwidth with the

tuning stub resonator. The stub length for the larger pad is 300 µm whereas the shorter stub requires only a 250 µm length.

The design of an active noise source requires an opposite approach compared to a low noise amplifier design. Instead of searching the minimum noise level of a gain stage the maximum is searched. Starting from the input referred noise circles the furthest location from input match noise optimum has to be searched. For the first cascode gain stage the noise circles for 170 and 230 GHz are plotted using an unmatched gain stage of Fig. 6 with a large inductive load. The minimum noise figures are found with rather real impedances between 20 - 30Ω - this time the region to be avoided (Fig. 7). In these designs, low real impedances were chosen for simplicity and a resistance of 10Ω was used for input termination.

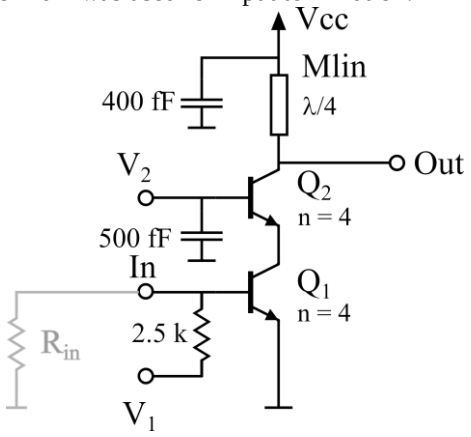

Fig. 6. Simplified cascode stage for the search of noise maximum of the first gain stage and with the input match resistor approach in gray.

Choosing a real source match instead of a reactive one is also justified by our wish for wide-band operation. Of course, reasonable gain and stable operation must be ensured when choosing appropriate input matching. In the noise source design with just an output signal, the term input matching is somewhat misleading and the first stage is just terminated with the chosen “input match” as shown in Fig. 6. The rest of the amplifier is designed to have high gain and wide bandwidth. Bandwidth of the amplifier mainly determines the bandwidth of the noise source.

The simulated S-parameters of the amplifier in the first amplifier-based noise source are plotted in Fig. 8. The output matching changes only slightly when the amplifier is turned off. The amplifier in the second noise source is identical except for the output transmission lines that have been slightly tuned to improve matching with the ground cut-out RF pad.

Micrographs of fabricated amplifier-based noise sources version 1 and 2 are shown in Fig. 9 and Fig. 10, respectively. The former was designed to have a larger gain and ENR at higher frequencies. Thus, this design utilizes the floating shield RF pad. The current consumption of both circuits is 19 mA and 15 mA in on-state and off-state, respectively, with a nominal supply voltage of 2.3 V.

Dependence of ENR to temperature was simulated to be about -0.03 dB/°C for all noise sources.

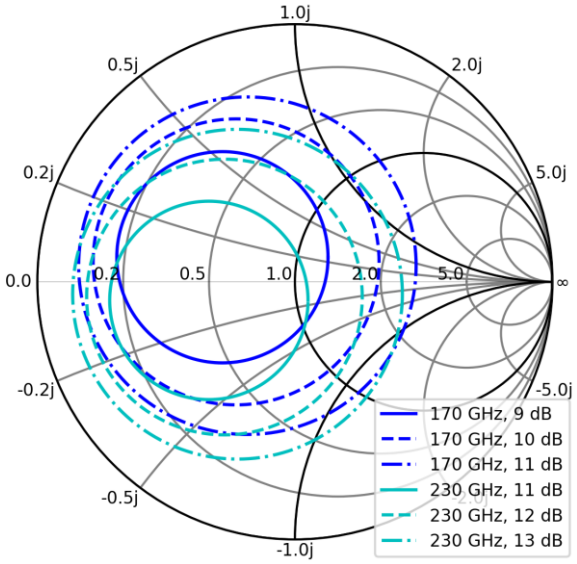

Fig. 7. Input matching of amplifier-based noise source using noise circle approach.

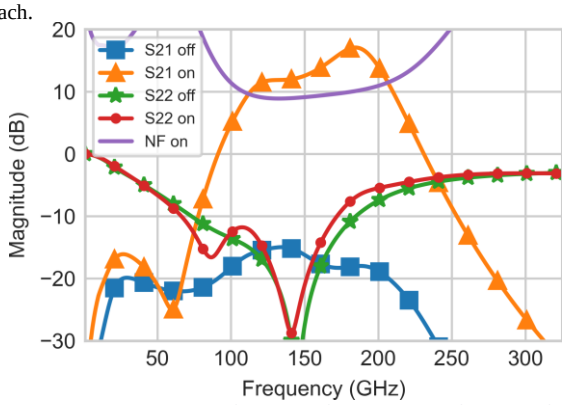

Fig. 8. Simulated S-parameters of the amplifier used in the first amplifier-based noise sources. Bias condition: 2.3-V supply voltage with 18 mA current.

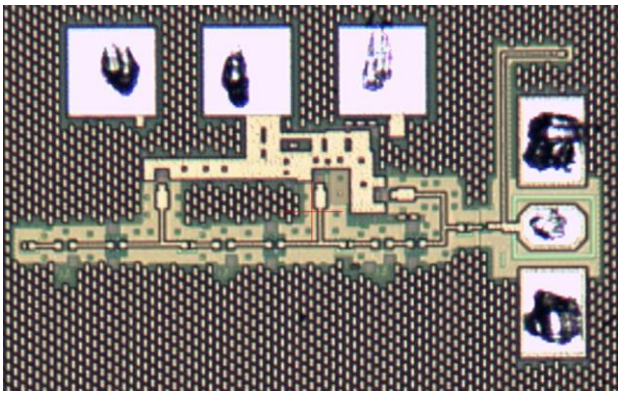

Fig. 9. Micrograph of first amplifier-based noise source. The chip area including pads is 650 µm × 375 µm.

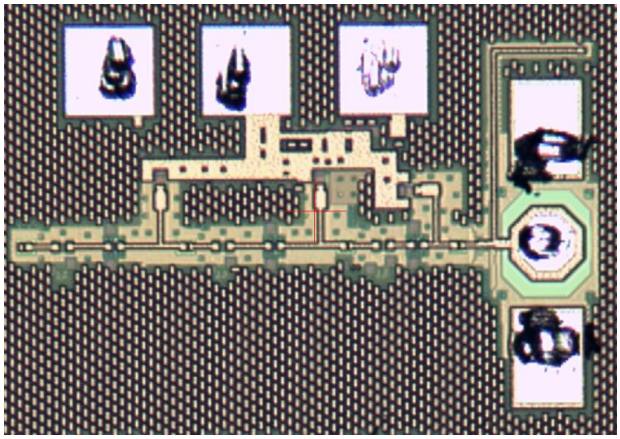

Fig. 10. Micrograph of the second amplifier-based noise source. The chip area including pads is 650 µm × 430 µm.

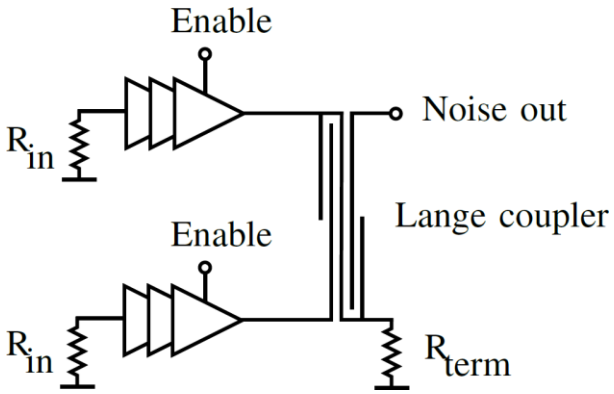

Fig. 11. Block diagram of the Lange coupler-based noise source.

B. *Lange coupler-based noise source*

To further improve the matching of the noise source a novel topology shown in Fig. 11. was developed. The circuit consists of two identical amplifiers connected to a Lange coupler with inputs terminated. The Lange coupler is used to improve the output matching similarly as is commonly used in balanced amplifiers. Due to the 90-degree phase shift of the Lange coupler, ideally the waves passing through the coupler reflecting off the amplifier outputs and passing back through the coupler experience 180-degree phase difference and cancel out at the output port. Reflected power is absorbed in the termination resistor R_{term}. Disabling the amplifiers changes the output reflection coefficient of the amplifiers but due to the Lange coupler the output matching of the circuit changes only minimally. The noise of the two amplifiers is uncorrelated and is divided equally in the Lange coupler to the output and termination R_{term} and ENR is identical to the ENR of a single amplifier. It should be noted that the Lange coupler design approach could be used just as well with avalanche diode-based noise source to improve the matching.

The Lange coupler coupling line length is 156 µm, width 2 µm and spacing 3 µm. Bottom metal layer was used as a ground plane and the signal lines are on top metal layer.

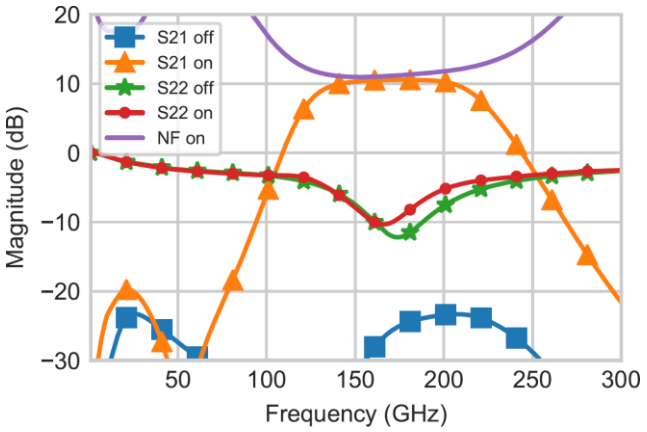

Fig. 12. Simulated S-parameters of a single amplifier used in the Lange coupler-based noise source. Bias condition: 2.3-V supply voltage with 18-mA current. Port 2 is the output port.

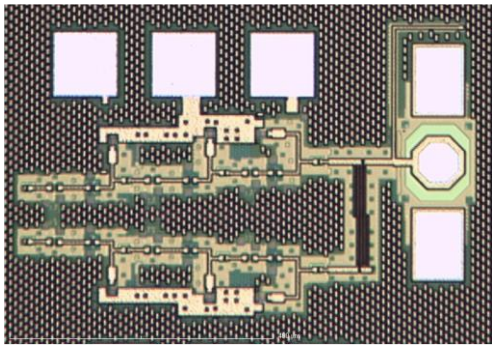

Fig. 13. Micrograph of the Lange coupler-based noise source. The chip area including pads is 700 µm × 510 µm.

Simulated S-parameters of a single amplifier that is employed in the Lange coupler-based noise source are presented in Fig. 12. The output matching of a single amplifier is at the best only around -10 dB, thus, adding the Lange coupler significantly improves the output matching of the noise source as will be shown in the next section.

Micrograph of the manufactured Lange coupler-based noise source is presented in Fig. 13. The simulated nominal supply voltage is 2.3 V with current consumption of 38 mA in on state and 30 mA in off state.

III. Measurements

A. *S-parameter measurements*

The S-parameters were measured using four different VNAs to achieve full coverage from 10 MHz to 300 GHz. Calibration was done in each case using LRRM method using an external calibration substrate. Measurement frequency ranges were partly overlapping and the differences in the setups cause some discontinuities. In the absolute scale these discontinuities are rather small.

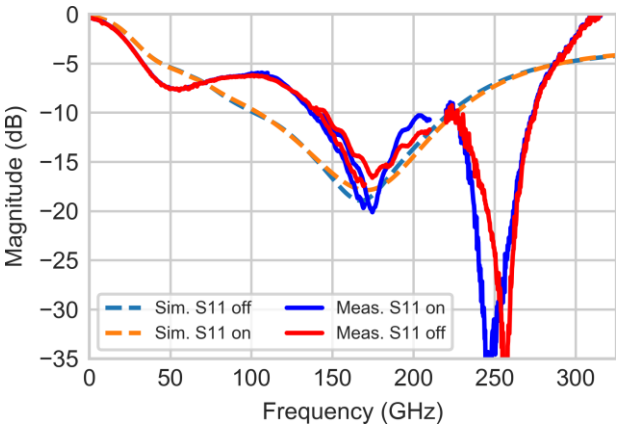

Fig. 14. Measured and simulated output matching of the first amplifier-based noise source both in on and off states. On-state bias condition: 2.3-V supply voltage with 21 mA current.

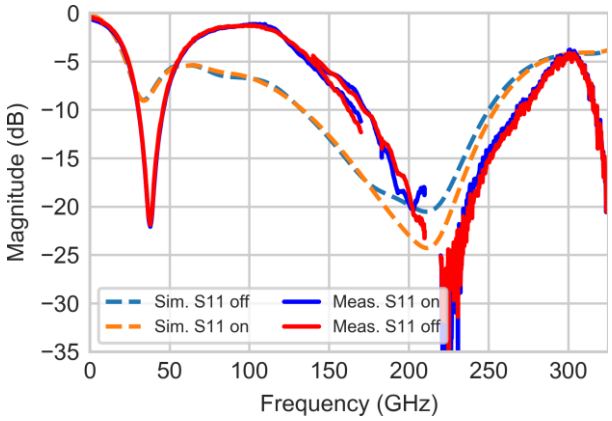

Fig. 15. Measured and simulated output matching of the second amplifier-based noise source both in on and off states. On-state bias condition: 2.3-V supply voltage with 21-mA current.

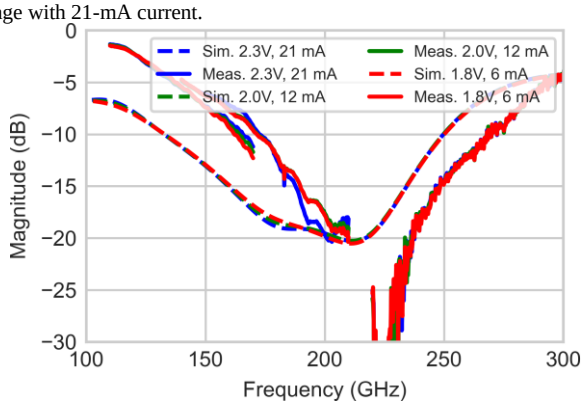

Fig. 16. Measured and simulated output matching of the second amplifier-based noise source in on-state with different supply voltages.

The measured and simulated output matching of the first amplifier-based noise source is shown in Fig. 14. The responses resemble qualitatively each other although there is quantitative difference. However, around 250 GHz the measured output matching differs significantly from the simulated one. This could be due to the modeling inaccuracies related to the floating shielded RF pad. The measured output matching is better than -10 dB between 175 to 280 GHz and better than -15 dB between 200 to 260 GHz. Both on- and off-states are shown and there is slightly worse matching in on-state but the difference between states is rather negligible.

For the second version of amplifier-based noise source, the measured and simulated matching is shown in Fig. 15. The measured characteristics are rather good, and the output matching is better than -10 dB in a rather wide band between 140 to 270 GHz. Again, the measured response is qualitatively rather like the simulated one although the quantitative difference is notable. Change in the output matching with different bias conditions was simulated to be minimal with all noise sources and this was found to be true in measurements (Fig. 16).

The measured and simulated output matching of the Lange coupler-based noise source is plotted in Fig. 17. The measurements agree relatively well with the simulations. The simulated output reflection coefficient is better than -12 dB from approximately 90 – 270 GHz in both on and off states.

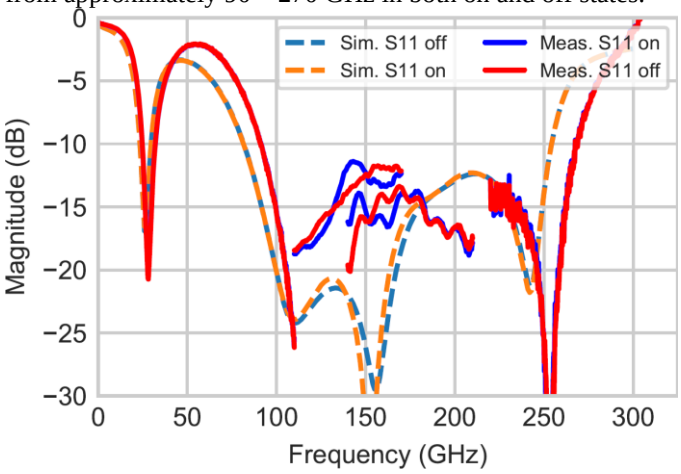

Fig. 17. Measured and simulated output matching of the Lange coupler-based noise source both in on and off states. On-state bias condition: 2.3-V supply voltage with 39-mA current.

The change in the output matching between on and off states is minimal. The relatively good match to simulations suggests that the Lange coupler at the output makes the output match more robust to modeling inaccuracies and fabrication tolerances.

B. Noise temperature measurements

The noise temperature was measured using three measurement systems from 110 to 170 GHz, 150 to 207 GHz and 210 GHz to 250 GHz. The measurement system for the 150 – 207 GHz frequency band is presented in Fig. 18. Isolator at the input is used to reduce reflections between the DUT and the subharmonic mixer. The noise is down converted with a subharmonic mixer and the power is measured with a noise figure analyzer. Noise temperature (Tr) and gain bandwidth product (*kBG*) of the noise receiver are determined using Y-factor method [7] and landing the RF probes on a thru line on an alumina calibration substrate. The noise figure includes the on-wafer probe between the DUT and the isolator. Solid state noise source Elva-1 ISSN-05 provides hot and cold noise temperatures for the calibration at 150-207 GHz band. Solid state noise source Elva-1 ISSN-06 was used at 110-170 GHz

band and an input terminated packaged amplifier was used at 210-250 GHz band. The output noise temperature of the packaged amplifier was calibrated with room temperature and liquid nitrogen absorber loads. Losses of the probe connected between the noise source and thru line are determined with the method described in [8]. Noise figures of the receivers are between 11-15 dB, 16-19 dB, and 14-17 dB at 110-170 GHz, 150-207 GHz, and 210-250 GHz, respectively. Output noise temperature Tout, and ENR of the noise source are calculated from the measured noise power P_{meas} using

$$T_{out} = \frac{P_{meas}}{kBG} - T_r \quad (1)$$

and

$$ENR_{dB} = 10\log_{10}\left(\frac{T_{out}-T_0}{T_0}\right) \quad (2)$$

where T_0 is the standard noise temperature 290 K. Mismatch effects are not taken into account in the calculation.

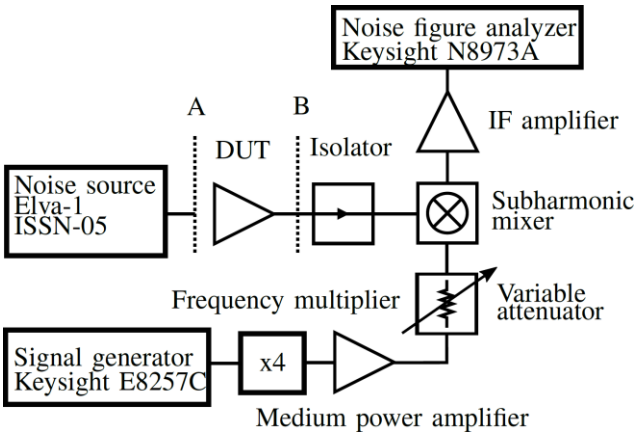

Fig. 18. ENR measurement setup.

ENR simulation and measurements of the amplifier-based noise source version 1, version 2 and Lange coupler-based noise sources are shown in Fig. 19, Fig. 20 and Fig. 21 respectively. In both amplifier-based devices the noise increases rapidly up to 120 GHz after which the noise ENR level is rather constant and then peaks at around 210 GHz. The measured ENR is slightly higher than simulated and the response is shifted toward higher frequencies. Mismatch between the noise source and the isolator at the receiver input can also cause some inaccuracy as the mismatch is not compensated in the measurement. The ENR level is rather dependent on supply voltage and in both cases the ENR variation difference between 1.8, 2.0 and 2.3 V supply is around 10 - 13 dB. The Lange coupler-based noise source ENR matches better to measurements, but it's also slightly shifted to higher frequencies.

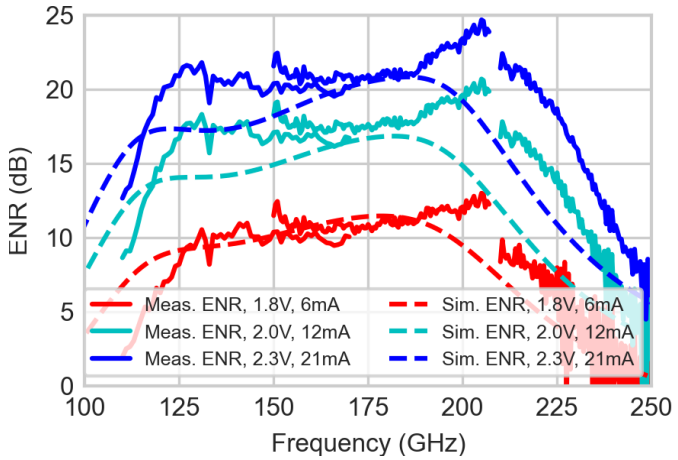

Fig. 19. Measured and simulated ENR of the first amplifier-based noise source with three different bias conditions.

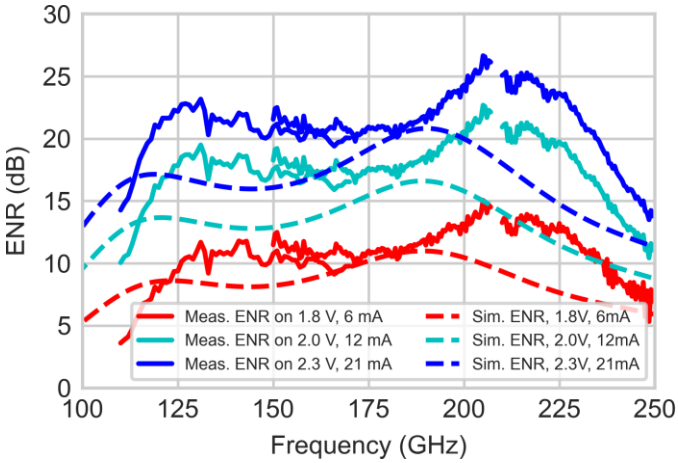

Fig. 20. Measured and simulated ENR of the second amplifier-based noise source with three different bias conditions.

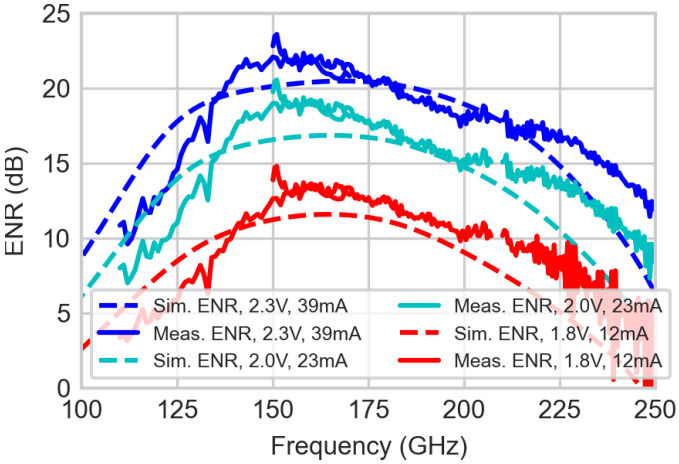

Fig. 21. Measured and simulated ENR of the Lange coupler-based noise source with three different bias conditions.

Table I Comparison of millimeter-wave noise sources

Technology	Topology	Supply current (mA)	Supply Voltage (V)	Frequency (GHz)	ENR (dB)	Return loss (dB)	Ref
packaged	waveguide with isolator	60	28	110-170	12 ± 3	14	[14]
silicon IMPATT diode	waveguide	50-100	18-28	110-170	12 ± 2	-	[15]
GaAs Schottky diode	waveguide	6	16	170-220	4-10	>2.5	[5]
BiCMOS Schottky diode	in-situ	7	6	130-260	15-20	-	[4]
InP HEMT	waveguide LNA	20	-	145-185	12-15	-	[7]
SiGe BiCMOS	switched avalanche diode	5	12	54-70	19	>10	[12]
SiGe BiCMOS	schottky diode	7	-	130-325	5-20	-	[8]
SiGe BiCMOS	p-i-n diode	2	11	1-40	19-36	-	[13]
SiGe BiCMOS	three-stage cascode amplifier	21	2.3	120-220 145-220	20-25 20-25	>7 >10	this work
SiGe BiCMOS	three-stage cascode amplifier	21	2.3	118-235 172-235	20-27 20-27	>2 >10	this work
SiGe BiCMOS	three-stage cascode amplifier with Lange coupler	39	2.3	125-235	15-22	>12	this work

IV. Conclusion

In this paper, we presented the design methodology for wideband input terminated millimeter-wave amplifier based noise sources and demonstrated the operation of SiGe BiCMOS amplifier based noise sources for the first time. The amplifier based noise sources are suitable for both on-chip in situ calibration as well as external noise sources for defining for example an amplifier noise figure. The amplifier-based noise-source design approach is readily applicable to other MMIC technologies since typically a noise model is available for LNA design.

Performance of millimeter-wave noise sources operating are gathered in Table I. All three noise sources have tunable ENR and the amplifier-based noise sources can be designed for low voltage operation. The three-stage single-ended cascade amplifier based noise sources achieve high ENR values above 20 dB from 120 to 220 GHz. However, for both single-ended noise sources the output matching is considerably much narrower limiting the usable range of the two noise sources. To overcome this, we proposed a novel Lange coupler based noise source which can operate at a very wide bandwidth as the measured output matching is better than -12 dB from 90 to 260 GHz. Furthermore, the Lange coupler at the output makes the output match more robust to modeling inaccuracies as well as fabrication tolerances and is suitable for other noise source topologies and technologies.

References

[1] M. Kärkkäinen, M. Kantanen, S. Caujolle-Bert, M. Varonen, R. Weber, A. Leuther, M. Seelmann-Eggebert, A. Alanne, P. Jukkala, T. Närhi, and K. A. I. Halonen, "MHEMT G -Band Low-Noise Amplifiers," *IEEE Trans. Terahertz Sci. Technol.*, vol. 4, no. 4, pp. 459-468, July 2014.

[2] S. T. Brown, S. Desai, W. Lu, and A. B. Tanner, "On the Long-Term Stability of Microwave Radiometers Using Noise Diodes for Calibration," *IEEE Trans. Geosci. Remote Sens.*, Vol. 45, No. 7, pp. 1908-1920, July 2007.

[3] A. Colliander, L. Ruokokoski, J. Suomela, K. Veijola, J. Kettunen, V. Kangas, A. Aalto, M. Levander, H. Greus, and M. T. Hallikainen, J. Lahtinen,"Development and Calibration of SMOS Reference Radiometer," *IEEE Trans. Geosci. Remote Sens.*, vol. 45, No. 7, pp. 1967-1977, July 2007.

[4] J. C. Azevedo Gonçalves, H. Ghanem, S. Bouvot, D. Gloria, S. Lépilliet, G. Ducournau, C. Gaquière, and F. Danneville, "Millimeter-Wave Noise Source Development on SiGe BiCMOS 55-nm Technology for Applications up to 260 GHz," *IEEE Trans. Microw. Theory Techn.*, vol. 67, no. 9, pp. 3732–3742, Sep. 2019.

[5] N. Ehsan, J. Piepmeier, M. Solly, S. Macmurphy, J. Lucey, and E. Wollack, "A robust waveguide millimeter-wave noise source," in *2015 Proc. EuMC*, Sep. 2015, pp. 853–856.

[6] F. Alimenti, G. Tasselli, C. Botteron, P. Farine, and C. Enz, "Avalanche microwave noise sources in commercial 90-nm cmos technology," *IEEE Trans. Microw. Theory Techn.*, vol. 64, no. 5, pp. 1409–1418, 2016.

[7] C. R. Parashare, P. P. Kangaslahti, S. T. Brown, S. Padmanabhan, A. B. Tanner, O. Montes, D. E. Dawson, T. C. Gaier, S. C. Reising, V. D. Hadel, T. P. Johnson, and X. Bosch-Lluis, "Noise sources for internal calibration of millimeter-wave radiometers," in *Proc. IEEE 13th Microw. Radiometry Remote Sens. Environ. (MicroRad)*, March 2014, pp. 157–160.

[8] H. Ghanem et al., "Modeling and Analysis of a Broadband Schottky Diode Noise Source Up To 325 GHz Based on 55-nm SiGe BiCMOS Technology," *IEEE Trans. Microw. Theory Techn.*, vol. 68, no. 6, pp. 2268-2277, June 2020

[9] G. Mamola, and M. Sannino, "Source mismatch effects on measurements of linear two-port noise temperatures," *IEEE Trans. Instrum. Meas.*, vol. 24, no. 3, pp. 239-242, Sept. 1975.

[10] H. T. Friis, "Noise figure of radio receivers," *Proceedings of I.R.E.*, vol. 32, no. 7, pp. 419-422, July 1944.

[11] R. T. Webster, A. J. Jr. Slobodnik, G. A. Roberts, "Determination of InP HEMT noise parameters and S-parameters to 60 GHz," *IEEE Trans. Microw. Theory Techn.*, vol. 43, no. 6, pp. 1216-1225, June 1995.

[12] C. T. Coen, M. Frounchi, N. E. Lourenco, C. D. Y. Cheon, W. L. Williams, and J. D. Cressler, "A 60-GHz SiGe radiometer calibration switch utilizing a coupled avalanche noise source," *IEEE Microw. Wireless Compon. Lett.*, vol. 30, no. 4, pp. 417–420, Apr. 2020.

[13] F. Alimenti, G. Simoncini, G. Brozzetti, D. Dal Maistro, and M. Tiebout, "Millimeter-Wave Avalanche Noise Sources Based on p-i-n Diodes in 130 nm SiGe BiCMOS Technology: Device Characterization and CAD Modeling," *IEEE Access*, vol. 8, pp. 178976–178990, 2020.

[14] "D-Band Noise Source with Faraday Isolator," https://www.eravant.com/110-to-170-ghz-12-db-enr-wr-06-waveguide-d-band-noise-source-with-faraday-isolator

[15] "Precision Calibrated Noise Sources," http://elva-1.com/products/a40036

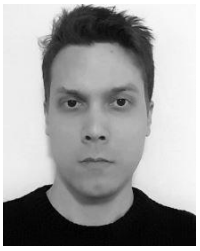

Henrik Forstén received the M.Sc. degree in electrical engineering from Aalto University, Espoo, Finland, in 2016. He is currently working as a Research Scientist with VTT Technical Research Centre of Finland, Espoo. His current research interest includes millimeter-wave integrated circuit design.

Jan H. Saijets was born in Stockholm, Sweden in 1971. He received M.S. and Ph.D. degrees in electrical engineering from the Helsinki University of Technology (Nowadays Aalto University) in 1998 and 2007, respectively.

From 1996 to 1998, he was a Research Assistant with VTT Electronics laboratory. Since 1998 he worked as a Research Scientist in VTT Microelectronics and since 2008 he has been a Senior Scientist in MilliLab VTT millimeter waves and antennas team. He is the author of 30 articles, and 4 inventions. His research interest includes millimeter wave IC design, integrated passive devices, micro-electro-mechanical-switches and RF MOSFET modeling.

Mikko Kantanen received the M.Sc., Lic.Sc., and D.Sc. degrees in Electrical Engineering from Aalto University (formerly Helsinki University of Technology), Espoo, Finland 2001, 2006, and 2017, respectively.

Since 2001 he has worked in MilliLab, VTT Technical Research Centre of Finland Ltd., Espoo, Finland, currently as a Senior Scientist. His research interests include millimeter-wave integrated circuit design, millimeter-wave measurements, and millimeter-wave systems.

Dr. Kantanen is a recipient of a 47th European Microwave Conference Microwave Prize and a co-recipient of an Asia-Pacific Microwave Conference 2006 Prize.

Mikko Varonen received the M.Sc., Lic.Sc., and D.Sc. (with distinction) degrees in electrical engineering from Aalto University (formerly, Helsinki University of Technology), Espoo, Finland, in 2002, 2005, and 2010, respectively. In 2011, he was a NASA Postdoctoral Program Fellow with the Jet Propulsion Laboratory (JPL), California Institute of Technology (Caltech), Pasadena, CA, USA. In 2012, he was a Post-Doctoral Researcher and the Academy of Finland Post-Doctoral Researcher with the Department of Micro- and Nanosciences, Aalto University from 2013 to 2016. During his Post-Doctoral Fellowship, he was a Visiting Scientist with the JPL, Electrical Engineering Department, Caltech, and the Fraunhofer Institute of Applied Solid-State Physics, Freiburg, Germany. He is currently a Senior Scientist and an Academy of Finland Research Fellow with the VTT Technical Research Centre of Finland, Espoo. His current research interests include the development of millimeter-wave integrated circuits using both silicon and compound semiconductor technologies for applications ranging from astrophysics and earth remote sensing to millimeter-wave communications.

Dr. –Ing Mehmet Kaynak received his B.S degree from Electronics and Communication Engineering Department of Istanbul Technical University (ITU) in 2004, took the M.S degree from Microelectronic program of Sabanci University, Istanbul, Turkey in 2006 and received the PhD degree from Technical University of Berlin, Berlin Germany in 2014. He joined the technology group of IHP Microelectronics, Frankfurt (Oder), Germany in 2008. From 2008 to 2015, he has led the MEMS development at IHP. From 2015 to 2020, he had served as the the department head of Technology at IHP.

Petri Piironen was born in Kuopio, Finland, on November 22, 1965. He received his Dipl.Eng. (M.Sc.), Licentiate of Technology, and Doctor of Science (Technology) degrees in electrical engineering from the Helsinki University of Technology, TKK (now Aalto University), Espoo, Finland, in 1990, 1992, and 1999, respectively.

From 1988 to 1994, he was with the HUT Radio Laboratory, working as a Research Assistant and Research Engineer. From 1994 to 1995, he was a Research Engineer at the Microwave Equipment and Technology Section of the European Space Research and Technology Centre (ESTEC), European Space Agency (ESA), Noordwijk, The Netherlands. In 1996, he was a Senior Scientist with the Millimetre Wave Laboratory of Finland—ESA External Laboratory (MilliLab). From 1997 to 1998, he was with the Millimeter Wave Group of the TKK Radio Laboratory as a Research Engineer. Since 1998, he has been with ESTEC RF Payloads and Technology Division as a microwave engineer. He supervises research and development activities in solid-state microwave and millimeter-wave functions and equipment for space applications.